

# A New Parameter $F$ to Classify Cellular Automata Rule Table Space and a Phase Diagram in $\lambda - F$ Plane

Sunao Sakai and Megumi Kanno

*Faculty of Education, Yamagata University, Yamagata, 990-8560, Japan*

---

## Abstract

It is shown that for the  $N$ -neighbor and  $K$ -state cellular automata, the class II, class III and class IV patterns coexist at least in the range  $\frac{1}{K} \leq \lambda \leq 1 - \frac{1}{K}$ . The mechanism which determines the difference between the pattern classes at a fixed  $\lambda$  is found, and it is studied quantitatively by introducing a new parameter  $F$ . Using the parameter  $F$  and  $\lambda$ , the phase diagram of cellular automata is obtained for 5-neighbor and 4-state cellular automata.

PACS: 89.75.-k Complex Systems

---

## 1 Introduction

Cellular automata (CA) has been one of the most studied fields in the research of complex systems. Various patterns has been generated by choosing the rule tables. Wolfram[1] has classified these patterns into four rough categories: class I (homogeneous), class II (periodic), class III (chaos) and class IV (edge of chaos). The class IV patterns have been the most interesting target for the study of CA, because it provides us with an example of the self-organization in a simple system and it is argued that the possibility of computation is realized by the complexity at the edge of chaos[2,3,4].

A more detailed classification of CA, has been carried out mainly for the elementary cellular automata (3-neighbor and 2-state CA)[5,6], in which the pattern is studied quite accurately for each rule table. However the number of rule table in  $N$ -neighbor and  $K$ -state cellular automata grows like  $K^{K^N}$ . Therefore except for a few smallest combinations of the  $N$  and  $K$ , the numbers of the rule tables become so large that studies of the CA dynamics for

---

<sup>1</sup> E-mail: sakai@e.yamagata-u.ac.jp

all rule tables are impossible even with the fastest supercomputers.

On the other hand the rule table of edge of chaos is rare in the whole CA rule table space, therefore it is important to find a set of parameters by which the pattern classes could be classified, and to determine a phase diagram of CA in these parameter space, even if it is a qualitative one.

Langton has introduced  $\lambda$  parameter and argued that as  $\lambda$  increases the pattern class changes from class I to class II and then to class III. And in many cases, class IV behavior is observed between class II and class III patterns[7,3,8]. The  $\lambda$  parameter represents rough behavior of CA in the rule table space, but finally does not sufficiently classify the quantitative behavior of CA. It is well known that different pattern classes coexist at the same  $\lambda$ . Which of these pattern classes is chosen, depends on the random number. The reason or mechanism for this is not yet known; we have no way to control the pattern classes at fixed  $\lambda$ . And the transitions between a periodic to chaotic pattern classes are observed in a rather wide range of  $\lambda$ . In Ref.[8], a schematic phase-diagram was sketched. However a vertical axis was not specified. Therefore, it is has been thought that more parameters are necessary to arrive at a more quantitative understanding of the rule table space of the CA.

In this article, we will report a mechanism which discriminates the pattern classes at a fixed  $\lambda$ . The mechanism is closely related to the structure of the rule tables and is expressed by the numbers of rules which breaks strings of quiescent state. For N-neighbor and K-state CA, it is found that in the region  $1/K \leq \lambda \leq 1 - 1/K$ , the class II, class III and class IV pattern classes coexist.

This property is studied quantitatively by introducing a new parameter  $F$ , which is taken to be orthogonal to  $\lambda$ . In the region  $1/K \leq \lambda \leq 1 - 1/K$ , the maximum of  $F$  correspond to class III rule tables while minimum of  $F$ , to class II or class I rule tables. Therefore the transition of the pattern classes takes place somewhere between these two limits without fail. If we determine the region of  $F$ , where the transitions of the pattern classes take place, we could obtain the phase diagram in  $\lambda - F$  plane.

The determination of the phase diagram is carried out for 5-neighbor and 4-state CA. In this case, phase boundary is not sharp but has some range in  $\lambda - F$  plane. The region has a gentle slope as a function of  $\lambda$ , and extends over the range  $0.2 \leq \lambda \leq 0.8$ . This means that for this CA the edge of chaos could be found at least in this range in  $\lambda$ .

In section 2, we will briefly summarize our notations and present a key discovery, which leads us to the understanding of the structure of the rule table and pattern classes. It strongly suggested that the rules which break strings of the quiescent states play an important role for the pattern classes.

In section 3, we classify rule tables according to the destruction and construction of strings of the quiescent states, and carry out the replacements of the rules to change the chaotic pattern class into periodic one and vice versa while keeping  $\lambda$  fixed. The reason why the patten classes changes by the replacements is discussed, and we will show that in the region  $1/K \leq \lambda \leq 1 - 1/K$ , the change of the pattern classes takes place without fail by the

replacements.

In section 4, the result obtained in section 3 is studied quantitatively by introducing a new parameter  $F$ . Using  $F$  and  $\lambda$ , we determine the phase diagram in the  $\lambda - F$  plane for 5-neighbor and 4-state CA.

Section 5 is devoted to conclusions and discussions.

## 2 Summary of CA and a key discovery

### 2.1 Summary of Cellular Automata

In order to make our arguments concrete, we focus mainly on the one-dimensional 5-neighbor and 4-state CA in the following, however, the qualitative conclusions hold true for other CAs. This point will be discussed in subsections 3.2.

We will briefly summarize our notation of CA[1,3]. In our study, the site consists of 150 cells having the periodic boundary condition. The states are denoted as  $s(t, i)$ . The  $t$  represents the time step which takes an integer value, and the  $i$  is the position of cells which range from 0 to 149. The  $s(t, i)$  takes values 0, 1, 2, and 3, and the state 0 is taken to be the quiescent state. The set of the states  $s(t, i)$  at the same  $t$  is called the configuration.

The configuration at time  $t + 1$  is determined by that of time  $t$  by using following local relation,

$$s(t + 1, i) = T(s(t, i - 2), s(t, i - 1), s(t, i), s(t, i + 1), s(t, i + 2)). \quad (1)$$

The set of the mappings

$$T(\mu, \nu, \kappa, \rho, \sigma) = \eta, (\mu, \nu, \text{etc.} = 0, 1, 2, 3) \quad (2)$$

is called the rule table. The rule table consists of  $4^5$  mappings, which are selected from a total of  $4^{1024}$  elements.

The  $\lambda$  parameter is defined as[3]

$$\lambda = \frac{N_h}{1024}, \quad (3)$$

where  $N_h$  is the number in which  $\eta$  in Eq.2 is not equal to 0. In other words the  $\lambda$  is the probability that the rules do not select the quiescent state in next time step. In the following we set the rule tables randomly with the probability  $\lambda$ . We choose  $1024 - N_h$  rules randomly, and set  $\eta = 0$  in the right hand side of Eq. 3. For the rest of the  $N_h$  rules, the  $\eta$  picks up the number 1, 2, 3 randomly.

The initial configurations are also set randomly.

The time sequence of the configurations is called a pattern. The patterns are classified roughly into four classes established by Wolfram[1]. It has been known that as the  $\lambda$  increases the most frequently generated patterns change from homogeneous (class I) to periodic (class II) and then to chaotic (class III), and at the region between class II and class III, the edge of chaos (class IV) is located.

## 2.2 Correlation between pattern classes and rules which break strings of quiescent state at a fixed $\lambda$

In order to find the reason why the different pattern classes are generated with the same  $\lambda$ , we have started to collect rule tables of different pattern classes, and tried to find the differences between them. We have fixed at  $\lambda = 0.44$  ( $N_h = 450$ ), because at this point the chaotic, edge of chaos, and periodic patterns are generated with a similar ratio. By changing the random number, we have gathered a few tens of the rule tables and classified them into chaotic, edge of chaos, and periodic ones.

In this article, a pattern is considered the edge of chaos when its transient length[3] is longer than 3000 time steps.

First, we study whether or not the pattern classes are sensitive to the initial configurations. We fix the rule table and change the initial configurations. The details of the patterns depend on the initial configurations, but the pattern classes are not changed[1]. Thus the difference of the pattern classes is due to the differences in the rule tables, and the target of our inquiry has to do with the differences between them.

For a little while, we do not impose a quiescent condition (QC)[3],  $T(0, 0, 0, 0, 0) = 0$ , because without this condition, the structure of the rule table becomes more transparent. This point will be discussed at the footnote 4 in section 4.

After some trial and error, we have found a strong correlation between the pattern classes and the QC. For class II patterns, the probability of the rule table, which satisfies the QC is much larger than that of the class III patterns. This correlation has suggested that the rule  $T(0, 0, 0, 0, 0) = h$ ,  $h \neq 0$ , which breaks the string of the quiescent states with length 5, pushes the pattern toward chaos. We anticipate that the similar situation will hold for the strings of quiescent states with length 4.

We go back to the usual definitions of CA. In the following we discuss CA under QC,  $T(0, 0, 0, 0, 0) = 0$ . We study the correlation between the number of the rules of Eq.4 and the pattern classes:

$$T(0, 0, 0, 0, i) = h, \quad T(i, 0, 0, 0, 0) = h, \quad (i, h = 1, 2, 3). \quad (4)$$

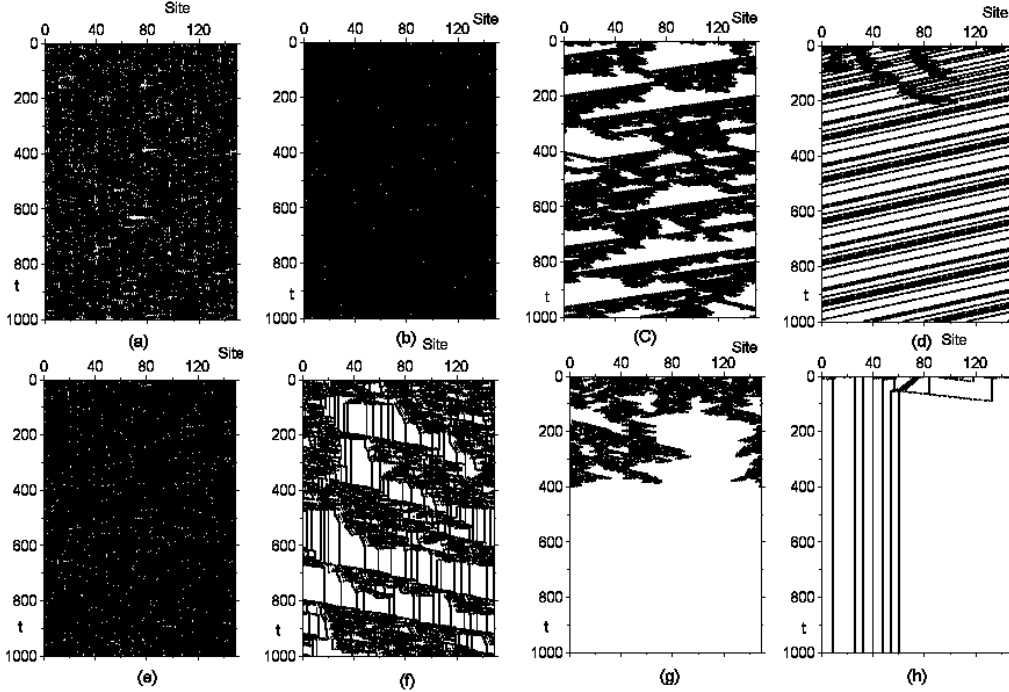


Fig. 1. The pattern classes at  $\lambda = 0.44$ . The quiescent state is shown by white dot, while other states are indicated by black point. Fig.1(a) corresponds to  $N_4 = 4$ , Fig.1(b), Fig.1(c), and Fig.1(d), to  $N_4 = 3$ , Fig.1(e), Fig.1(f), and Fig.1(g), to  $N_4 = 2$ , and Fig.1(h) corresponds to  $N_4 = 1$ .

These rules break length 4 strings of the quiescent states, and will also push the pattern toward chaos<sup>2</sup>. We denote the total number of rules of Eq.4 in a rule table as  $N_4$ . We have collected 30 rule tables and grouped them by the number  $N_4$ . We have 4 rule tables with  $N_4 \geq 4$ , 13 rule tables with  $N_4 = 3$ , 9 rule tables with  $N_4 = 2$  and 4 rule tables with  $N_4 \leq 1$ . When  $N_4 \geq 4$ , all rule tables generate chaotic patterns, while when  $N_4 \leq 1$ , only periodic ones are generated. At  $N_4 = 3$  and  $N_4 = 2$ , chaotic, edge of chaos, and periodic patterns coexist. Examples are shown in the Fig.1. The coexistence of three pattern classes at  $N_4 = 3$  is seen in Fig.1(b), Fig.1(c) and Fig.1(d) and that of  $N_4 = 2$  is exhibited in Fig.1(e), Fig.1(f) and Fig.1(g).

The strong correlation between  $N_4$  and the pattern classes has been observed in this case too, as anticipated. These discoveries have provided us with a key hint leading us to the hypothesis that the rules, which break strings of the quiescent states, will play a major role in the pattern classes.

<sup>2</sup> Similar ideas had been noticed by Wolfram and Suzudo with the arguments of the unbounded growth[1] and expandability[9].

### 3 Structure of rule table and pattern classes

#### 3.1 Structure of rule table and replacement experiment

In order to test the hypothesis of the previous section, we classify the rules into four groups according to the operation on strings of the quiescent states. In the following, Greek characters in the rules represent groups 0, 1, 2, 3 while Roman, represent groups 1, 2, 3.

Group 1:  $T(\mu, \nu, 0, \rho, \sigma) = h$ .

The rules in this group break strings of the quiescent states.

Group 2:  $T(\mu, \nu, 0, \rho, \sigma) = 0$ .

The rules of this group conserve them.

Group 3:  $T(\mu, \nu, i, \rho, \sigma) = 0$ .

The rules of this group develop them.

Group 4:  $T(\mu, \nu, i, \rho, \sigma) = l$ .

The rules in this group do not affect string of quiescent states in next time step.

The sum of the numbers of the group 1 and group 2 rules is 256, while that of group 3 and group 4 rules is 768. The number of each group of rules included in the rule table is determined mainly by the probability  $\lambda$ , therefore it suffers from fluctuation due to randomness.

The group 1 rules are further classified into five types according to the length of string of quiescent states, which they break. These are shown in Table 1.

Table 1

The classification of the rules in group 1.

type	Total Number	Name	Replacement
$T(0, 0, 0, 0, 0) = h$	1	D5	RP5,RC5
$T(0, 0, 0, 0, i) = h$	3	D4	RP4,RC4
$T(i, 0, 0, 0, 0) = h$	3		
$T(0, 0, 0, i, \sigma) = h$	12	D3	RP3,RC3
$T(i, 0, 0, 0, m) = h$	9		
$T(\mu, j, 0, 0, 0) = h$	12		
$T(\mu, j, 0, 0, m) = h$	36	D2	RP2,RC2
$T(i, 0, 0, l, \sigma) = h$	36		
$T(\mu, j, 0, l, \sigma) = h$	144	D1	RP1,RC1

The D5 rule is always excluded from rule tables by the quiescent condition.

Our hypothesis presented at the end of the section 2 is expressed more quantitatively as follows; the numbers of the D4, D3, D2, and D1 rules shown in Table 1 will mainly determine the pattern classes.

In order to test this hypothesis we artificially change the numbers of these rules in Table 1 while keeping the  $\lambda$  fixed. For D4 rules, we carry out the

replacements defined by the following equations,

$$\begin{aligned}
T(0, 0, 0, 0, i) = h &\rightarrow T(0, 0, 0, 0, i) = 0, \\
\text{or } T(i, 0, 0, 0, 0) = h &\rightarrow T(i, 0, 0, 0, 0) = 0, \\
T(\mu, \nu, j, \rho, \sigma) = 0 &\rightarrow T(\mu, \nu, j, \rho, \sigma) = l,
\end{aligned} \tag{5}$$

where except for  $h$ , the groups  $\mu, \nu, \rho, \sigma, j$  and  $l$  are selected randomly. Similarly the replacements are generalized for D3, D2, and D1 rules, which are denoted as RP4 to RP1 in Table 1. They change the rules of group 1 to that of group 2 together with group 3 to group 4 and are expected to push the rule table toward the periodic direction.

The reverse replacements for D4 are

$$\begin{aligned}
T(0, 0, 0, 0, i) = 0 &\rightarrow T(0, 0, 0, 0, i) = h, \\
\text{or } T(i, 0, 0, 0, 0) = 0 &\rightarrow T(i, 0, 0, 0, 0) = h, \\
T(\mu, \nu, j, \rho, \sigma) = l &\rightarrow T(\mu, \nu, j, \rho, \sigma) = 0,
\end{aligned} \tag{6}$$

which will push the rule table toward the chaotic direction. In this case, the groups  $h, \mu, \nu, j, \rho,$  and  $\sigma$  are selected randomly. Similarly we introduce the replacements for D3, D2, and D1, which will be called RC4 to RC1 in the following.

By the replacement of RP4 to RP1 or RC4 to RC1, we change the numbers of the rules in Table 1 while keeping the  $\lambda$  fixed. We denote these numbers  $N_4, N_3, N_2,$  and  $N_1$  for D4, D3, D2, and D1 rules, respectively. The examples of the replacement experiments are shown in Fig.2.

The rule table of Fig.2(a) is obtained randomly with probability  $\lambda = 0.6$ .

Table 2

The numbers of the rules and the replacements for each figures shown in Fig.2

Figure	$N_4$	$N_3$	$N_2$	$N_1$	RP4	RP3	RP2	RP1
Fig.2(a)	3	22	53	96	0	0	0	0
Fig.2(b)	0	14	53	96	3	8	0	0
Fig.2(c)	0	13	53	96	3	9	0	0
Fig.2(d)	0	12	53	96	3	10	0	0
Fig.2(e)	1	7	53	96	2	15	0	0
Fig.2(f)	1	6	53	96	2	16	0	0
Fig.2(g)	2	1	53	96	1	21	0	0
Fig.2(h)	2	0	53	96	1	22	0	0

At  $\lambda = 0.6$  most of the randomly created rule tables generate chaotic patterns. Fig.2(b) is obtained by the 3 RP4s and 8 RP3s, and the numbers of the rules become  $N_4 = 0$  and  $N_3 = 14$ , respectively. These numbers are summarized in Table 2. By this replacements, Fig.2(b) shows an edge of chaos behavior.

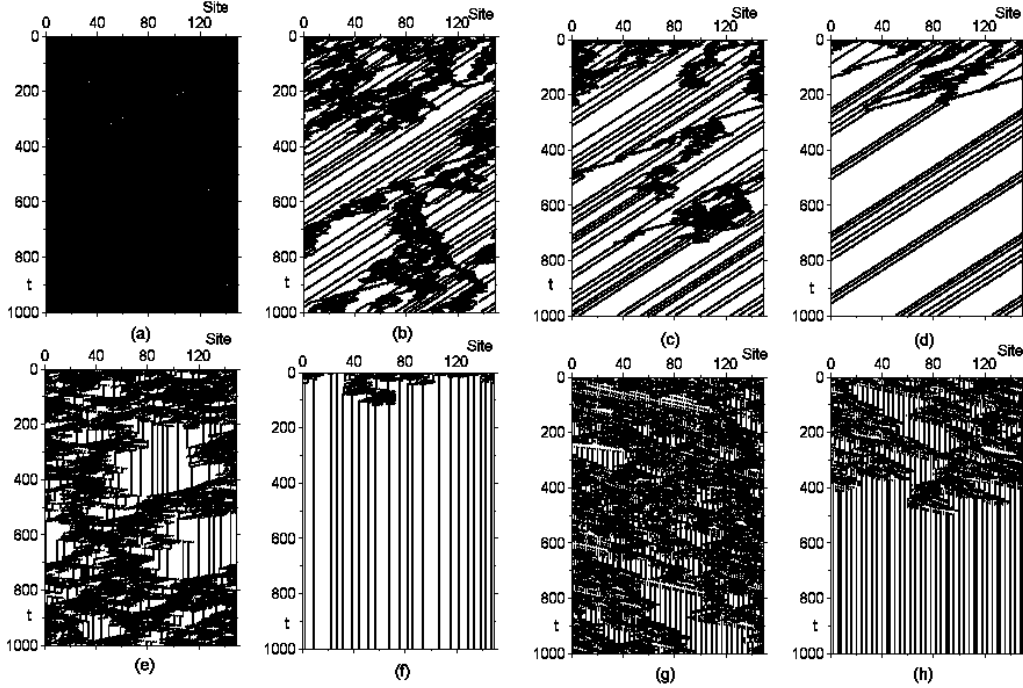


Fig. 2. Example of the replacement experiments at  $\lambda = 0.6$ . Fig.2(a) is obtained randomly with probability  $\lambda = 0.6$ , by the method explained in subsection 2.1. Fig.2(b) to Fig.2(h) are obtained by the replacements of the rules of Fig.2(a), which are summarized in Table 2.

When  $N_4 = 0$ , until  $N_3 = 22$  to  $N_3 = 15$ , the rule tables generate chaotic patterns. Fig.2(c) is obtained by one more RP3 replacements for Fig.2(b) rule table. It shows a periodic pattern with a rather long transient length. One more replacement of RP3 for the Fig.2(c) rule table is shown in Fig.2(d), where the transient length becomes shorter.

Similar replacement experiments for  $N_4 = 1$  and  $N_4 = 2$  cases are shown in Fig.2(e), Fig.2(f), and Fig.2(g), Fig.2(h), respectively. In these cases, until  $N_3 \geq 8$  and  $N_3 \geq 2$ , rule tables generate class III patterns at  $N_4 = 1$  and  $N_2 = 2$ , respectively. In these examples, edges of chaos are observed between classes III and II behaviors.

For each  $\lambda = 0.8, 0.75, 0.7, 0.6, 0.5, 0.4, 0.3$  and  $0.2$  point, we have carried out a several hundreds to a few thousands replacement experiments. In these replacements, we have succeeded in changing chaotic rule tables to a periodic ones by the replacements of RP4 to RP2, and vice versa by RC4 to RC2. For the replacements RP4, RP3 and RP2, we have observed no example that the rule table moves to chaotic direction. The converse is true for RC4, RC3 and RC2. Exceptions are observed only in the replacements RP1 and RC1, which will be discussed in section 4.



### 3.2 Chaotic and periodic limit at fixed $\lambda$ in $N$ -neighbor and $K$ -state CA

Let us study the effects of the replacements theoretically in the  $N$ -neighbor and  $K$ -state CA. In this general case too, the rule tables are classified into four groups. We denote the number of the group 1 rules as  $N(g1)$ , and similarly for the numbers of the other groups. These numbers satisfy the following sum rules.

$$\begin{aligned} N(g2) + N(g3) &= K^N(1 - \lambda), & N(g1) + N(g4) &= K^N \lambda, \\ N(g1) + N(g2) &= K^{N-1}, & N(g3) + N(g4) &= K^{N-1}(K - 1). \end{aligned} \quad (7)$$

The individual numbers  $N(gi)$  are determined by the probability  $\lambda$ . They are summarized in the Table 3. They suffer from fluctuations due to random number, however in this subsection, we neglect the fluctuations.

The replacements to decrease the number of the group 1 rule while keeping Table 3

The classification of  $N$ -neighbor and  $K$ -state CA rules into four groups. The  $\mu_i$  represent 0 to  $K-1$  and  $h, i$  and  $l$ , 1 to  $K-1$ .

	rule	$N(gi)$
group 1	$T(\mu_1, \mu_2, \dots, 0, \dots, \mu_N) = h$	$K^{N-1} \lambda$
group 2	$T(\mu_1, \mu_2, \dots, 0, \dots, \mu_N) = 0$	$K^{N-1}(1 - \lambda)$
group 3	$T(\mu_1, \mu_2, \dots, i, \dots, \mu_N) = 0$	$K^{N-1}(K - 1)(1 - \lambda)$
group 4	$T(\mu_1, \mu_2, \dots, i, \dots, \mu_N) = l$	$K^{N-1}(K - 1) \lambda$

the  $\lambda$  fixed are given by,

$$\begin{aligned} N(g1) &\rightarrow N(g1) - 1, & N(g2) &\rightarrow N(g2) + 1 \\ N(g3) &\rightarrow N(g3) - 1, & N(g4) &\rightarrow N(g4) + 1 \end{aligned} \quad (8)$$

In the case of 5-neighbor and 4-state CA, they correspond to RP4 to RP1.

These replacements stop either when  $N(g1) = 0$  or  $N(g3) = 0$  is reached. Therefore when  $N(g1) \leq N(g3)$ , which corresponds to  $\lambda \leq (1 - \frac{1}{K})$  in  $\lambda$ , all the group 1 rules are replaced by the group 2 rules. In this limit, quiescent states at time  $t$  will never be changed, because there is no rule which converts them to other states, while the group 3 rules have a chance to create a new quiescent state in the next time step. Thus the number of quiescent states at time  $t$  is a non-decreasing function of  $t$ ; therefore, the pattern class should be class I (homogeneous) or class II (periodic), which we call periodic limit. Therefore the replacements of Eq.8 push the rule table toward the periodic limit.

Let us discuss the reverse replacements of Eq.8. In these replacements, if  $N(g2) \leq N(g4)$ , all group 2 rules are replaced by the group 1 rules, except for

the quiescent condition. In this extreme reverse case, all the quiescent states at time  $t$  are converted to other states in next time step, while group 3 rules create them at different places. Then this will most probably develop into chaotic patterns. This limit will be called chaotic limit, which is reached in the region  $\frac{1}{K} \leq \lambda$ . We should like to say that atypical rule table and initial condition might generate a periodic patterns even in this limit. But in this article, these exceptional cases are neglected.

Therefore in the following region,

$$\frac{1}{K} \leq \lambda \leq 1 - \frac{1}{K}, \quad (9)$$

all the rule tables are located between these two limit, and by the replacements of Eq. 8 and their reverse ones, the changes of the pattern classes take place without fail. This explains the validity of the hypothesis of previous section. And we have found a method to control the pattern classes at fixed  $\lambda$ .

#### 4 Phase diagram of 5-neighbor and 4-state CA in $\lambda$ - $F$ plane

In the previous section, we have found that rule table is located somewhere between chaotic limit and periodic limit, in the region  $\frac{1}{K} \leq \lambda \leq 1 - \frac{1}{K}$ . In order to express the position of the rule table quantitatively, we introduce new parameter  $F$ , which provides us with a new axis ( $F$ -axis) orthogonal to  $\lambda$ . Minimum of  $F$  is the periodic limit, while maximum of it corresponds to chaotic limit. In this section, we determine the parameter  $F$ , for 5-neighbor and 4-state CA.

As a first approximation, the parameter  $F$  is taken to be a function of the numbers of the rules D4, D3, D2 and D1, which have been denoted as  $N_4$ ,  $N_3$ ,  $N_2$  and  $N_1$ , respectively. We proceed to determine  $F(N_4, N_3, N_2, N_1)$  by applying simplest approximations and assumptions

We have observed in the replacement experiments, that the position of the rule table in  $F$  moves toward chaotic direction, when  $N_4$  or  $N_3$  or  $N_2$  increases. Examples are shown in Fig. 2 and Table 2. However for D1, replacements RP1 and RC1 sometimes look like random walk on  $F$ -axis, around the region where the transition of the pattern class is taken place<sup>3</sup>. Therefore  $F$  will be a complicated function of  $N_1$  and determination of it will be difficult.

However the number  $N_1$  is rather large, therefore we apply mean field approximation for  $N_1$ . We replace  $N_1$  by its average, and measure  $F$  from this

<sup>3</sup> The effect of D1 rule is to change an isolates quiescent state to other states in the next time step. This effects may easily be compensated by the creation of quiescent states by group 3 rules in one time step. This may be a reason that the replacements of RP1 and RC1 some times look like random walk.

background; namely the  $N_1$  dependence is dropped from  $F$  and take  $F = 0$  at  $N_4 = N_3 = N_2 = 0$ .

Here, we apply Taylor series expansion for  $F$  at this point, and approximate it by the linear terms in  $N_4$ ,  $N_3$  and  $N_2$ .

$$F(N_4, N_3, N_2) \simeq c_4 N_4 + c_3 N_3 + c_2 N_2. \quad (10)$$

where  $c_4 = \partial F / \partial N_4$ , similar for  $c_3$  and  $c_2$ . They represent the strength of the effects of the rules D4, D3, and D2 to push the rule table toward chaotic direction. This definition is symbolic, because  $N_4$  is discrete.

The measure in the  $F$  is still arbitrary. We fix it in the unit where the increase in one unit of  $N_4$  results in the change of  $F$  in one unit. This corresponds to divide  $F$  in Eq.10 by  $c_4$ , and to express it by the ratio  $c_3/c_4$  ( $r_3$ ) and  $c_2/c_4$  ( $r_2$ ).

Before we proceed to determine  $r_3$  and  $r_2$ , let us interpret the parameter  $F$  geometrically. Most generally, the rule tables are classified in 1024-dimensional space in this CA. The rule tables, at the boundary of the class III and class II pattern classes at fixed  $\lambda$ , form a hyper-surface in this space. We map the points on hyper-surface into 3-dimensional  $(N_4, N_3, N_2)$  space. They will be located in some region in the 3-dimensional space. We introduce a surface  $F(N_4, N_3, N_2) = \Phi$  in order to line up these points.  $F$ -axis is a normal line of the surface  $F(N_4, N_3, N_2) = \Phi$ . In Eq.10, we approximate it by a plane.

Our strategy to determine  $r_3$  and  $r_2$  is to find the regression plane in  $N_4$ ,  $N_3$ , and  $N_2$  space. It is equivalent to fix the  $F$ -axis in such a way that the projection of the distribution of transition points on  $F$ -axis, ( $F_{crit}$ ) looks as narrow as possible. The quality of our approximations and assumptions reflects the width of the distribution of  $F_{crit}$ .

In the least square method, our problem is formulated to find  $r_3$  and  $r_2$ , which minimize the quantity,

$$s(r_3, r_2) = \frac{1}{c_4^2} \sum_{i,j} (F_{crit}^i(N_4^i, N_3^i, N_2^i) - F_{crit}^j(N_4^j, N_3^j, N_2^j))^2, \quad (11)$$

where  $i$  and  $j$  label the rule tables on the hyper-surface mapped into 3-dimensional space. We solve the equations,  $\partial S / \partial r_3 = 0$  and  $\partial S / \partial r_2 = 0$ , which are

$$\begin{aligned} r_3 \sum_{i,j} (\delta N_3^{i,j})^2 + r_2 \sum_{i,j} \delta N_2^{i,j} \delta N_3^{i,j} &= - \sum_{i,j} \delta N_4^{i,j} \delta N_3^{i,j}, \\ r_3 \sum_{i,j} \delta N_3^{i,j} \delta N_2^{i,j} + r_2 \sum_{i,j} (\delta N_2^{i,j})^2 &= - \sum_{i,j} \delta N_4^{i,j} \delta N_2^{i,j}, \end{aligned} \quad (12)$$

where  $\delta N_4^{i,j} = N_4^i - N_4^j$ , similar for  $\delta N_3^{i,j}$  and  $\delta N_2^{i,j}$ .

By artificially carrying out the replacements of RP4, RP3 and RP2 or RC4, RC3 and RC2, we look for critical combinations of  $N_4$ ,  $N_3$ , and  $N_2$ , at which the change of the pattern classes are observed. The examples of the critical combinations are presented in the lines of Fig.2(b), Fig.2(e), and Fig.2(g) of Table 2.

The numbers of the critical combinations ( $N_{c^{tot}}$ ), which are used to determine  $r_3$  and  $r_2$  in Eq. 12, are summarized in the Table 4. The  $r_3$  and  $r_2$  are determined for each  $\lambda$ . Their results are also shown in Table 4, where the errors are estimated by the jackknife method.

The results show that the coefficients are positive, and satisfy the order,

$$c_4 > c_3 > c_2. \quad (13)$$

It means that the effects to move the rule table toward chaotic limit on the  $F$ -axis are stronger for the rules which break longer strings of the quiescent states.

The order in Eq.13 is understood by the following intuitive arguments. If six D4 rules are included in the rule table, the string of the quiescent states with length 5 will not develop. Similarly, if 33 D3 rules are present in the rule table, no length 4 string of the quiescent states could be made. These are roughly similar situations for pattern classes. Thus the strength of the D3 rules will be roughly equal to 6/33 of that of D4 rules, similar for the strength of the D2 and D1 rules <sup>4</sup>.

Using these results for  $r_3$  and  $r_2$ , we calculate  $F$ 's for each critical combination ( $F_{crit}$ ). For  $\lambda = 0.6$ , they are shown in Fig.3a for 101 data points. The number distributions of them are displayed in Fig.3b. From these 101 data, we calculate average,  $\langle F_{crit} \rangle$  and standard deviation  $\sigma$  of the distribution of  $F_{crit}$ . Similar calculations are carried out for other  $\lambda$  points. The results for  $\langle F_{crit} \rangle$ ,  $\langle F_{crit} \rangle \pm \sigma$  and maximum of  $F$  ( $F_{max}$ ) determined by the coefficients  $r_3$  and  $r_2$  are shown in the Fig.4. This is a phase diagram in  $\lambda - F$  plane.

The phase diagram is natural in the sense that as  $\lambda$  increases, the proportion of the chaotic rule table region increases in the total  $F$  range. The two lines  $\langle F_{crit} \rangle \pm \sigma$  in the figure, indicate that about 68% of the critical combinations are located in this region, if the normal distribution is assumed for

---

<sup>4</sup> If we do not impose the quiescent condition, Eq.13 becomes

$$c_5 > c_4 > c_3 > c_2.$$

Therefore the correlation between pattern classes and the existence of D5 rule is stronger than the correlation between those and the number of D4 rules. If we start our study within the quiescent condition, we may make a longer detour to find the hypothesis of section 2 and get the qualitative conclusion of section 3.

Table 4

The number of the critical combinations  $Nc^{tot}$  and the coefficients  $r_3$  and  $r_2$ .

$\lambda$		Relative Strength	Error	$Nc^{tot}$
0.2	$r_3$	0.1083	0.0020	119
	$r_2$	0.0153	0.0025	
0.3	$r_3$	0.1083	0.0028	90
	$r_2$	0.0069	0.0021	
0.4	$r_3$	0.1182	0.0074	58
	$r_2$	0.0165	0.0072	
0.5	$r_3$	0.1023	0.0047	61
	$r_2$	0.0262	0.0010	
0.6	$r_3$	0.1288	0.0019	101
	$r_2$	0.0216	0.0013	
0.7	$r_3$	0.1631	0.0063	92
	$r_2$	0.0342	0.0042	
0.75	$r_3$	0.1505	0.0114	92
	$r_2$	0.0419	0.0065	
0.8	$r_3$	0.1315	0.0168	89
	$r_2$	0.0420	0.0038	

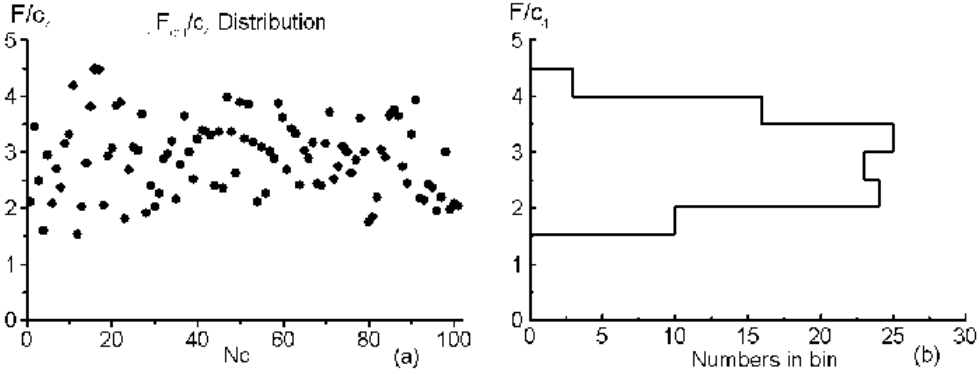


Fig. 3. Distribution of critical combinations  $F_{crit}$  at  $\lambda = 0.6$ . Fig.3a shows 101 individual  $F_{crit}$  points. We label these 101 points by  $Nc$ . In Fig.3b, number distribution of the critical combinations in the bin is displayed. The region of distribution of  $F_{crit}$  is divided into 6 bins.

$F_{crit}$ . We call this region as transition region. We think that the class II and class III patterns would not be separated by a line in  $\lambda - F$  plane. Because the transition region in Fig. 4 is a mapping of the hyper-surface, which separates the two pattern classes at a fixed  $\lambda$  in 1024 dimensional space, into the normal line of the regression plane in the 3-dimensional space. Therefore the two parameters will not be enough to draw the boundary by a line.

However we should like to notice that in spite of the simple approximations and assumptions, the  $F_{crit}$ s distribute within a rather narrow portion of total  $F$  range as shown in Fig. 4. At  $\lambda = 0.6$ , the total range of  $F$  is  $0 \leq F \leq 11.8$ . All the  $F_{crit}$  distribute within the region  $1.5 \leq F \leq 4.48$ , which is roughly 1/4 of the total region. The region  $\langle F_{crit} \rangle \pm \sigma$  occupies only about 11% of whole range of  $F$ . The similar situation is observed for the other  $\lambda$  points.

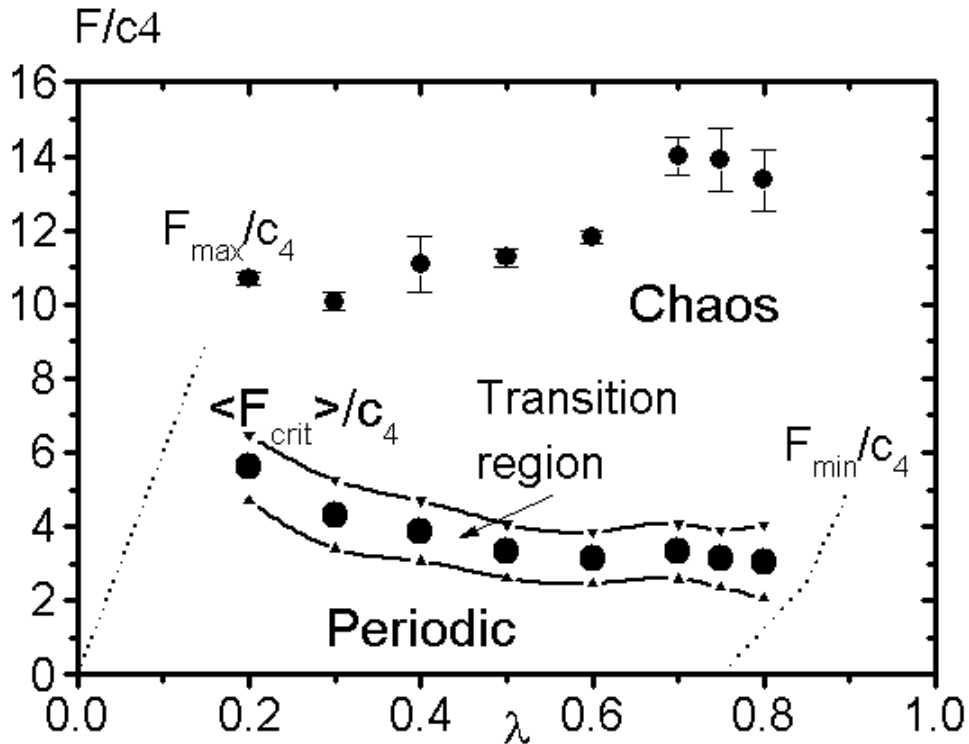


Fig. 4. Phase diagram of the 5-neighbor and 4-state cellular automata. The  $\langle F_{crit} \rangle / c_4$  and the  $F_{max} / c_4$  are shown with filled circle. The  $\langle F_{crit} \rangle / c_4 + \sigma$  is shown with down triangle and the  $\langle F_{crit} \rangle / c_4 - \sigma$ , with up triangle. They are joined by lines. A schematic sketch of  $F_{min}$  in  $0.75 \leq \lambda$ , and  $F_{max}$  in  $\lambda \leq 0.25$  are also shown by the dotted lines. They are drawn based on the arguments in the text.

The Fig.4 is still qualitative but rule table space of CA is classified much better by using  $\lambda$  and  $F$ . And it provides us with a deeper understanding of the structure of the CA rule table space. The existence of the transition region in  $0.2 \leq \lambda \leq 0.8$ , means that the edge of the chaos could be found at least in this region, which is rather wide range in  $\lambda$ .

Let us discuss the distribution of the rule tables around the transition region. All the class IV rule tables are located around transition region as Fig. 3 shows, but converse is not true. In this region, the three pattern classes coexist and the number densities of the class II plus class III rule table are considerably larger than that of class IV rule tables. Outside of the transition region, the probability of finding the class IV rule table decreases rapidly and the pattern classes began to be classified only by the position in the  $\lambda - F$  plane; in the  $\langle F_{crit} \rangle + \sigma \leq F$  region, class III rule tables dominates while in the  $F \leq \langle F_{crit} \rangle - \sigma$  region, class II or class I CA dominates. The similar distributions of the rule tables are observed at  $\lambda = 0.8, 0.75, 0.7, 0.5, 0.4, 0.3$  and  $0.2$ .

We proceed to the investigation of the end points of the transition region. In the subsection 3.2, we have find the region of  $\lambda$ , where both chaotic limit and

periodic limit coexist. In the 5-neighbor and K-state CA, it is  $1/4 \leq \lambda \leq 3/4$ .

In  $\lambda < 0.25$  region, not all the group 2 rules could be replaced by the group 1 rules. Therefore the maximum of  $N(g1)$  could not become 256, and it decreases to zero as  $\lambda$  approaches to zero. Then the maximum of  $F$ , ( $F_{max}$ ) also decreases to zero toward  $\lambda = 0$ .

Conversely in  $\lambda > 0.75$  region, not all the group 1 rules could be replaced by the group 2 rules. The minimum of  $N(g1)$  and therefore the minimum of  $F$ , ( $F_{min}$ ) could not become 0. The line  $F_{min}$  increases until  $\lambda = 1$ . In Fig.4, we have schematically shown the  $F_{max}$  and  $F_{min}$  lines with dotted lines.

The points where the transition region crosses the  $F_{min}$  and  $F_{max}$  lines determine the end points of the coexistence of the two limits, and also the end points of existence of the class IV rule tables. We have already found that the transition region is found in the region  $0.2 \leq \lambda \leq 0.8$ . Therefore the crossing points are outside of this region in the case of 5-neighbor 4-state CA.

## 5 Conclusions and discussions

At a fixed  $\lambda$ , the pattern classes of the CA could be controlled by the numbers of the group 1 rules, which has been denoted by  $N(g1)$ . The maximum of  $N(g1)(= K^{N-1} - 1)$  corresponds to chaotic limit, and  $N(g1) = 0$ , to the periodic limit. In the N-neighbor and K-state CA, these two limits exist in the region  $\frac{1}{K} \leq \lambda \leq 1 - \frac{1}{K}$ . Therefore in this  $\lambda$  region, we could control the pattern classes by changing  $N(g1)$  without fail. The method for it, is the replacements of Eq. 8. This provides us with a new method to obtain the rule table of edge of chaos. However, we should like to comment that the fluctuation due to the random number will make the statements less rigorous.

This property is studied quantitatively by introducing a new parameter  $F$ . The maximum of the  $F$  corresponds to the chaotic limit and minimum of it, the periodic limit. By changing the  $F$  using the replacements, we could find the region, where the transition of the class II and class III patterns takes place. Thus we could obtain the phase diagram of the CA in  $\lambda - F$  plane.

In this article, we have applied the analysis to 5-neighbor and 4-state CA. In this case the group 1 rules are further classified into 5 types as shown in Table 1, and the phase diagram is obtained in Fig.4. The transition region has a rather gentle slope as a function of  $\lambda$ , and it extends at least from  $\lambda = 0.2$  until  $\lambda = 0.8$ , which is wider than  $\frac{1}{4} \leq \lambda \leq 1 - \frac{1}{4}$ . This explains why the edge of chaos is found in the wide range in  $\lambda$  for this CA. It may be interesting whether or not the slope of the transition region depends on the models.

In the replacement experiments, we have found the edge of chaos (very long transient lengths) in many cases. The examples are shown in Fig.2. Sometimes they are observed in a rather wide range in  $N_3$  or  $N_2$ . This indicates that in

many cases, the transitions are second-order like. But the widths in the ranges of  $N_3$  or  $N_2$  are different from each other, and there are cases where the widths are less than one unit in the replacement of RP2 (first-order like). It is very interesting to investigate under what condition the transition becomes first-order like or second-order like. The mechanism of the difference in the nature of the transition is an open problem and may be studied by taking into account effects of group 2, 3, and 4 rules. In these studies another new parameters may be found and a more quantitative phase diagram may be obtained.

It is also interesting to compare the detailed dynamics of class IV CA at different points of rule table space in  $\lambda - F$  plane by applying Wuensche's method[6] or by using computational mechanics[5].

These issues together with finding the points where the transition region crosses  $F_{max}$  and  $F_{min}$  lines in Fig.4, and the nature of the phase transition at these points will be addressed in the forthcoming publications.

## References

- [1] S. Wolfram, Physica D 10(1984) 1-35.
- [2] S. Wolfram, Physica Scripta T9(1985) 170-185.
- [3] C.G.Langton, Physica D 42(1990) 12-37.
- [4] M. Mitchell, J.P.Crutchfield and P.T. Hraber, Santa Fe Institute Studies in the Science of Complexity, Proceedings Volume 19. Reading, MA., Addison-Wesley. online paper, <http://www.santafe.edu/~mm/paper-abstracts.html#dyn-comp-edge>.
- [5] J.E.Hanson and J.P.Crutchfield, Physica D 103(1997),169-189.
- [6] A. Wuensche, Complexity Vol.4/No.3(1999) 47-66.
- [7] C.G.Langton, Physica D 22(1986) 120-149.
- [8] W.LI, N.H.Packard and C.G.Langton, Physica D45(1990) 77-94.
- [9] T. Suzudo, Crystallisation of Two-Dimensional Cellular Automata, Complexity International, Vol. 6(1999). on line journal, <http://www.csu.edu.au/ci/vol06/suzudo/suzudo.html>. See appendix.